Supporting Information

Sheet-like and tubular aggregates of protein nanofibril-phosphate hybrid

Xiangsheng Han,[1,2] Lili Lv,[1,2] Mingjie Li,[1] Jun You,[1] Xiaochen Wu,[1,] and Chaoxu Li[1,2,*]*

[1]CAS Key Lab of Bio-based materials, Qingdao Institute of Bioenergy and Bioprocess Technology, Chinese Academy of Sciences, Songling Road 189, Qingdao 266101, P. R. China

[2]Center of Materials Science and Optoelectronics Engineering, University of Chinese Academy of Sciences, 9A Yuquan Road, Beijing 100049, China

*Corresponding Authors: C. Li (licx@qibebt.ac.cn); X. Wu (wuxc@qibebt.ac.cn).

Experimental

Materials. Bovine serum albumin (BSA) (Biotech Grade, purity > 96 %, molecular weight ~ 66.4 kDa) was bought from Sangon Biotech (Shanghai) Co., Ltd. Gelatin was from Bioroyee (Beijing) Biotechnology Co., Ltd. 1,2,3,4-Butane tetracarboxylic acid (99 %) were obtained from Aladdin Industrial Corporation. Thioflavin T (97 %) were from Macklin. Phosphotungstic acid (2 wt.%) were from Solarbio. Phosphate, ethanol and other reagents were obtained from Sinopharm Chemical Reagent Co. Ltd., China. Ultrapure water (resistivity: 18.2 MΩ cm^{-1}) was used throughout the experiments.

Aligning BSA nanofibrils into microtubes and nanosheets. Typically, 1.0 g of BSA was dissolved in 40 mL of phosphate buffer (pH 7.4). The phosphate concentration was tuned within 0-50 mM. After adding 60 mL of ethanol, the solution was incubated at 65 °C for 24 h and then at 25 °C for 2 days for fibrillation. After gradually reducing the temperature below 10 °C and standing for 6 h, the precipitates were collected and re-dispersed in *tert*-butanol for characterization.

Chemical fixation of aligned protein fibrils. Microtubes and nanosheets of protein nanofibrils were dispersed in *tert*-butanol. 1,2,3,4-Butane tetracarboxylic acid (0.5 wt.%) was added as the cross-linker, and incubated at 25 °C for 24 h. The products were washed with H_2O for 3 times, replaced with *tert*-butanol, lyophilized and stored at 4 °C for further usages.

Aligning BSA nanofibrils on substrates. The substrates of chemically reduced graphene oxide films, silica and brushite platelets were pre-cooled in liquid nitrogen for 10 min, and quickly immersed into a dispersion of BSA nanofibrils in ethanol solution (60 vol.% of ethanol, 50 mM of phosphate, pH 7.4) at 20 °C. After incubation for 24 h, the substrates were taken out, immersed in *tert*-butanol, lyophilized and stored at 4 °C for characterization.

Apatite hybridization of microtubes. BSA microtubes were dispersed in *tert*-butanol, 1,2,3,4-butane tetracarboxylic acid (0.5 wt.%) was added as the cross-linker, and incubated at 25 °C for 24 h to get the chemical fixed microtubes. Then $CaCl_2$ was added to reach a concentration of 50 mM, and incubated at room temperature for 6 h. The product was washed with H_2O for > 3 times, replaced with *tert*-butanol, lyophilized and stored at 4 °C for further usages.

Gelatin hybridization of microtubes. The chemically fixed BSA microtubes were mixed with 1-Ethyl-3-(3'-dimethylaminopropyl) carbodiimide hydrochloride (EDC, 8 mM) and N-Hydroxysuccinimide (NHS, 2 mM) at room temperature for 1 h. 2 mL of gelatin solution (5 wt.%) was then added and incubated for 12 h. After washing with H_2O for 3 times and incubating at 4 °C for 1 h, the product was immersed in ammonium sulfate solutions (20 wt.%) for 12 h and stored at 4 °C for further usages.

Attaching magnetic particles on microtubes. For the preparation of Fe_3O_4 nanoparticles,[S1] 1,6-Hexanediamine (6.5 g), anhydrous sodium acetate (2.0 g) and $FeCl_3 \cdot 6H_2O$ (1.0 g) were added into glycol (30 mL) and stirred vigorously at 50 °C to give a transparent solution. The solution was then transferred into a Teflon lined autoclave and reacted at 200 °C for 6 h. The magnetite nanoparticles were then rinsed with water and ethanol 3 times, dried at 50 °C to get the Fe_3O_4 nanoparticles. 20 mg of Fe_3O_4 nanoparticles (~ 25 nm) were dispersed in 400 μL of phosphate buffer (pH 7.4, 50 mM) and 600 μL of ethanol, then added dropwise into 20 mL of BSA nanofibrils (1 wt.%, pH 7.4, 60 vol.% of ethanol, 50 mM of phosphate) with vigorously stirring. The mixture was cooling from room temperature (~ 25 °C) to below 10 °C and standing for 24 h to get the magnetic microrods.

Cell proliferation on BSA aligned microtubes. The cross-linked BSA microtubes were sterilized at 120 °C for 6 h. Hela cells were seeded on the microtubes with a density of 3×10^3 cells per well in 96-well plates. After culturing at 37 °C in a CO_2 incubator with 5 % CO_2 supply for 3 days, the microtubes

were washed with PBS buffer for 3 times and immersed in staining solution consisting of Calcein-AM (2 μM) and Propidium Iodide (4 μM) for 30 min at 37 °C. Staining solution was removed, microtubes were washed twice with PBS and imaged using Olympus BX51 fluorescence microscopy (excited at 490nm). For comparison, Hela cells cultured on coverslips were conducted as control.

Fibrillation of lysozyme.[S2] Briefly, lysozyme (≥ 90 %, from chicken egg white, Sigma-Aldrich) was dissolved in H_2O and then adjusted to pH 2.0 and 2.0 wt.%. Fibrillation was performed by incubating at 60 °C for 96 h under mildly stirring.

Fibrillation of silk nanofibrils. Bombyx mori cocoons were collected from Shandong, China. Silk fibroin was regenerated following a sequential procedure of degumming, dissolving, and dialysis to a concentration of ~ 5 wt.% as described in the literature.[S3] For the fibrillation of silk fibroin, ethanol was added into the aqueous solution of silk fibroin to achieve the silk concentration of 0.2 wt.% and ethanol composition of 7 vol.%, the solution was incubated at 25 °C and pH 9.5 for 2 days to assemble silk nanofibrils.

Characterization. Morphologies were characterized by Hitachi H-7650 transmission electron microscopy (TEM, Japan) and JEOL 7401 emission scanning electron microscopy (FESEM, Japan, acceleration voltage of 5 kV). BSA nanofibrils oriented micro-tubes were replaced with *tert*-butanol, lyophilized, sputter-coated with platinum and imaged using FESEM. For TEM imaging, the micro-tubes were included in epoxy resin at 60 °C for 24 h. After permeation, samples were cut into slices (70 nm in thickness) using a microtome and translated onto grid. Contrast of microtubes was achieved by negative staining through adding a droplet of phosphotungstic acid (2 wt.%) onto the grid, and let the staining act over a period of 15 min, any excess of staining agent was removed again by a filter paper. Microscopic photographs were acquired using Olympus BX51 fluorescence microscopy (Japan) and Olympus Fluo ViewTM FV1000 laser scanning confocal microscopy (Japan). Observed with

excitation wavelength at 330-385 nm for intrinsic protein fluorescence and 460-490 nm for Thioflavin T binding fluorescence. The fluorescence emission spectra were obtained on a Hitachi F-4600 Spectrofluorometer (Japan) equipped with a 150 W xenon lamp as the excitation source. UV-Vis spectrophotometric analyses were performed on a DU800 UV-vis spectrophotometer in the range of 200-800 nm. X-ray diffraction (XRD) measurements were taken on a Bruker D8 ADVANCE X-ray diffractometer (Germany) using Cu Kα (λ = 1.5406 Å) radiation. X-ray scattering experiments were performed on a Bruker-AXS NanoSTAR instrument (Germany) with Cu-Kα microsource at 30W, with the scattering vector windows of 3.6-20 nm^{-1}. Dried samples were encapsulated and fixed on the sample holder. Circular Dichroism (CD) measurements were carried out on a BioLogic MOS-450 spectropolarimeter (France) using a cuvette with a path length of 1 mm at 25 °C. Fourier transform infrared (FT-IR) analysis was performed on a Nicolet 6700 FT-IR spectrometer (American) using the KBr pellets method, and analyzed using Peakfit 4.0 on amide Ⅲ band (1220-1330 cm^{-1}). Atomic force microscope (AFM) in tapping mode was performed on Agilent 5400 at a scan rate of 1 Hz equipped with silicon nitride cantilevers (Bruker). Nanosheets of BSA nanofibrils were fixed with 1,2,3,4-butane tetracarboxylic acid, washed with H_2O, dropped onto freshly cleaved mica surface, and dried naturally to acquire the AFM samples.

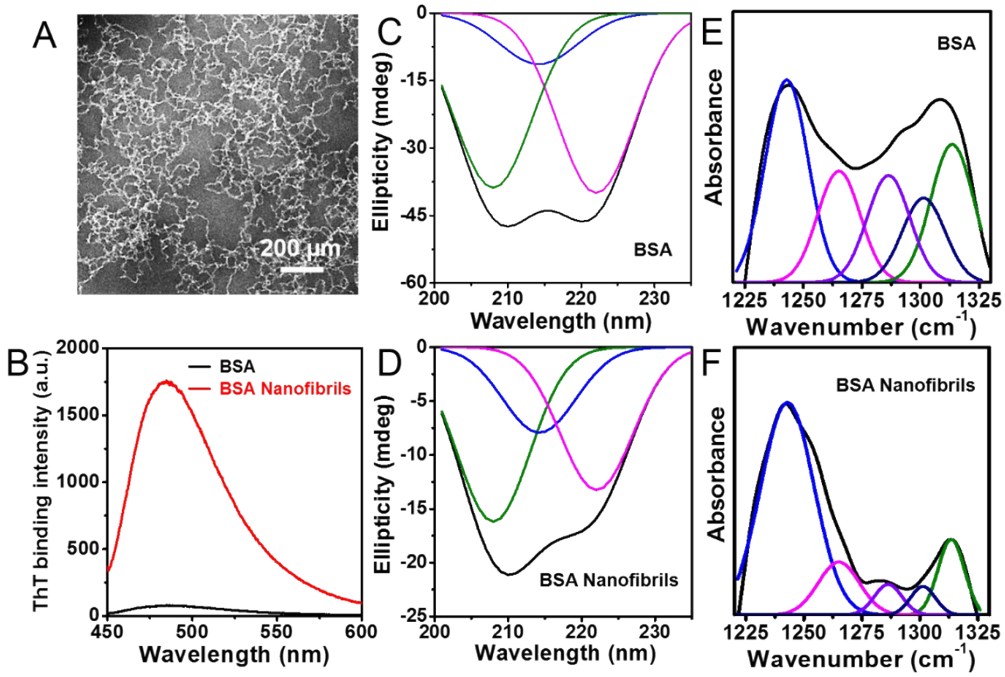

Figure S1. (A) TEM image of BSA nanofibrils. (B) Thioflavin T binding fluorescence spectra of BSA upon fibrillation, excited at 440 nm. (C-D) Far-UV circular dichroism and (E-F) FTIR spectra of BSA and BSA nanofibrils.

The CD spectrum of native BSA is typical of a well-defined protein structure, with the presence of two minima at 222 and 208 nm associated with the existence of predominant α-helical structure. After the thermal treatment, a decrease in the ellipticity was observed, indicating a reduction in the α-helical content and the formation of disordered conformations or β-aggregate structures. The minimum at ~ 215 nm associating with β-sheet structure was also increased, confirming the formation of amyloidal "β-sheets".

For the FTIR spectra, the amide III band for BSA and BSA nanofibrils was fitted to the following peaks: 1242 cm^{-1} (β-sheets), 1264 cm^{-1} (unordered structures), 1285 cm^{-1} (β-turns), 1301 cm^{-1} (α-helices), and 1313 cm^{-1} (α-helices). After the fibrillation, the amounts of α-helices and unordered structures decreased, while the ratio of β-sheets increased, presented the conformational transition from α-helical structures to β-sheet structures.

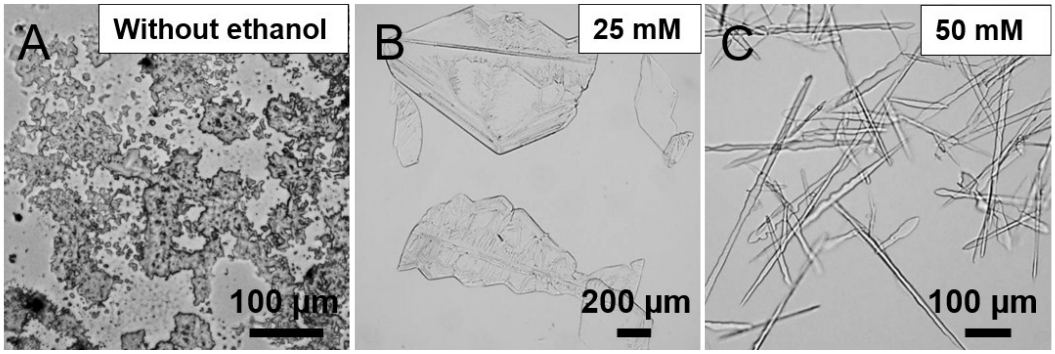

Figure S2. Optical images of phosphate crystals formed by cooling from 25 °C to 5 °C. (A) 50 mM of sodium phosphate buffer (pH 7.4). (B) Sodium phosphate buffer (25 mM, pH 7.4) with 60 vol.% ethanol. (C) Sodium phosphate buffer (50 mM, pH 7.4) with 60 vol.% ethanol.

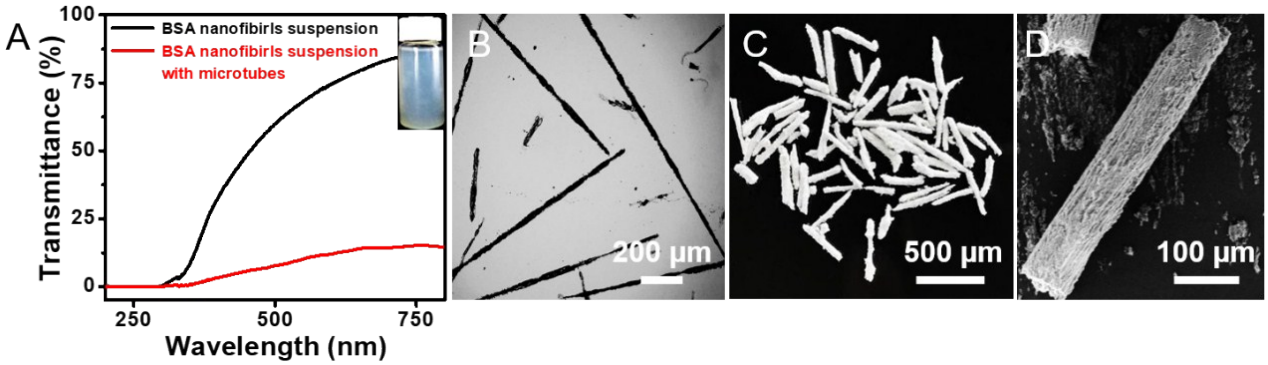

Figure S3. Characterization of phosphate crystal rods with shell of BSA fibrils. (A) UV-vis transmittance before and after phosphate crystallization. (B) Microphotograph. (C) Visual observation. (D) SEM image.

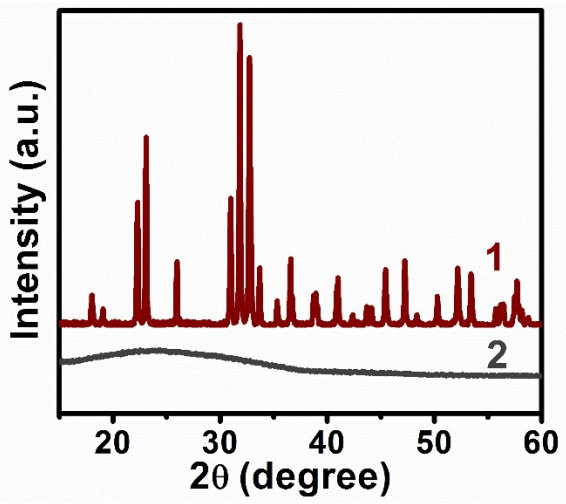

Figure S4. XRD patterns of (1) phosphate crystal rods with shell of BSA fibrils and (2) cross-linked BSA microtubes after washing off phosphate crystal rods.

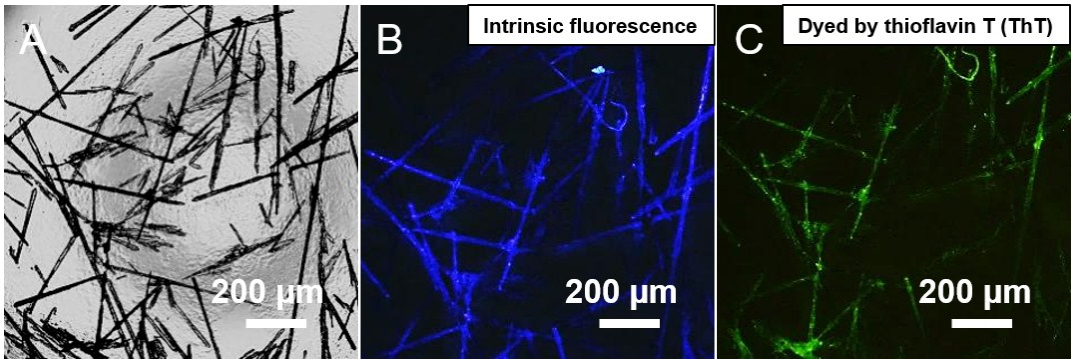

Figure S5. Phosphate crystal rods with shell of BSA fibrils. (A) Microphotograph. (B) Intrinsic fluorescence excited at 330-385 nm. (C) ThT binding fluorescence excited at 460-490 nm.

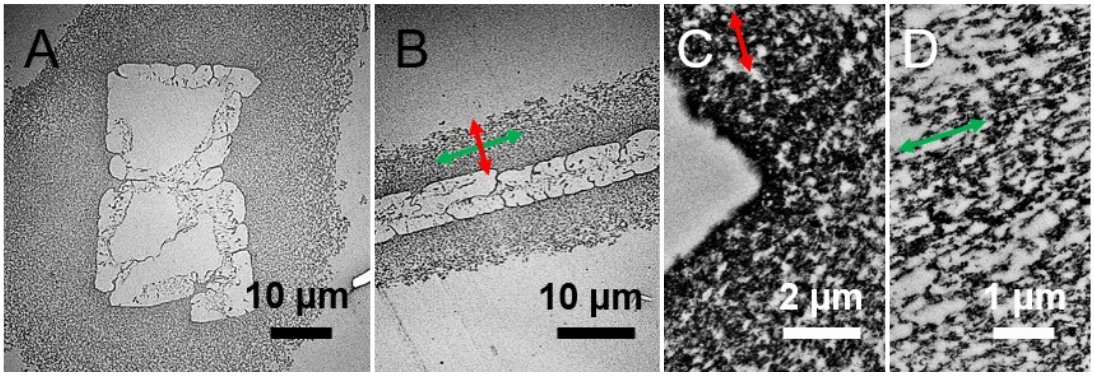

Figure S6. TEM images of transverse (A, C) and longitudinal (B, D) sections of phosphate crystals with shell of BSA fibrils.

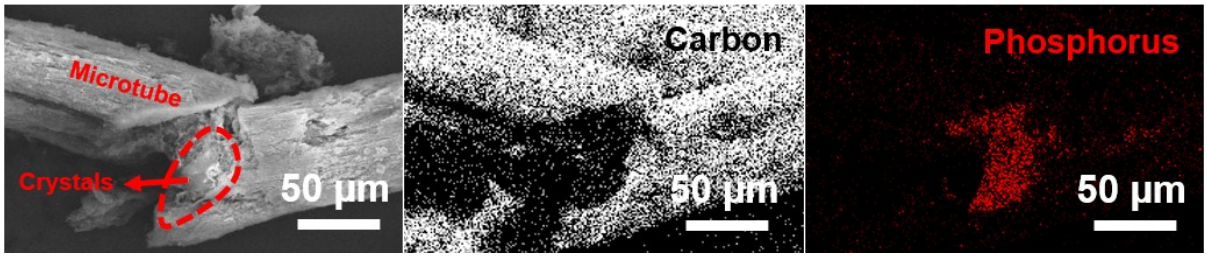

Figure S7. Energy-dispersive X-ray spectroscopy mapping of broken phosphate crystal rod with shell of BSA fibrils, revealing phosphate crystal core and protein shell.

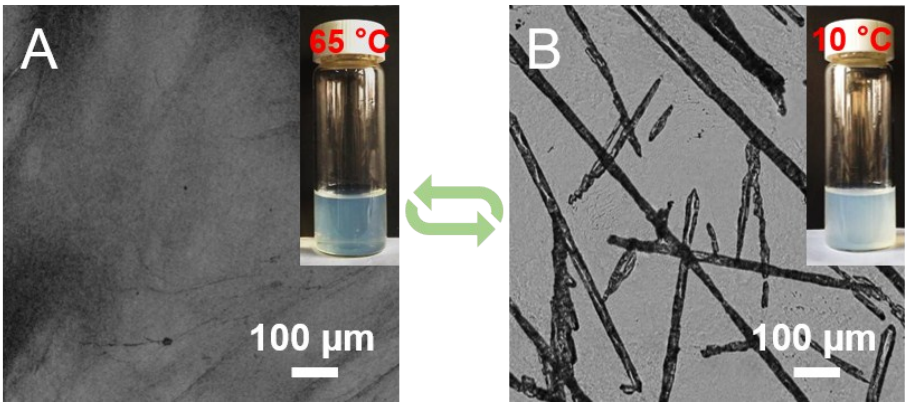

Figure S8. Reversible formation of phosphate crystals with shell of BSA fibrils by heating (A) and cooling (B).

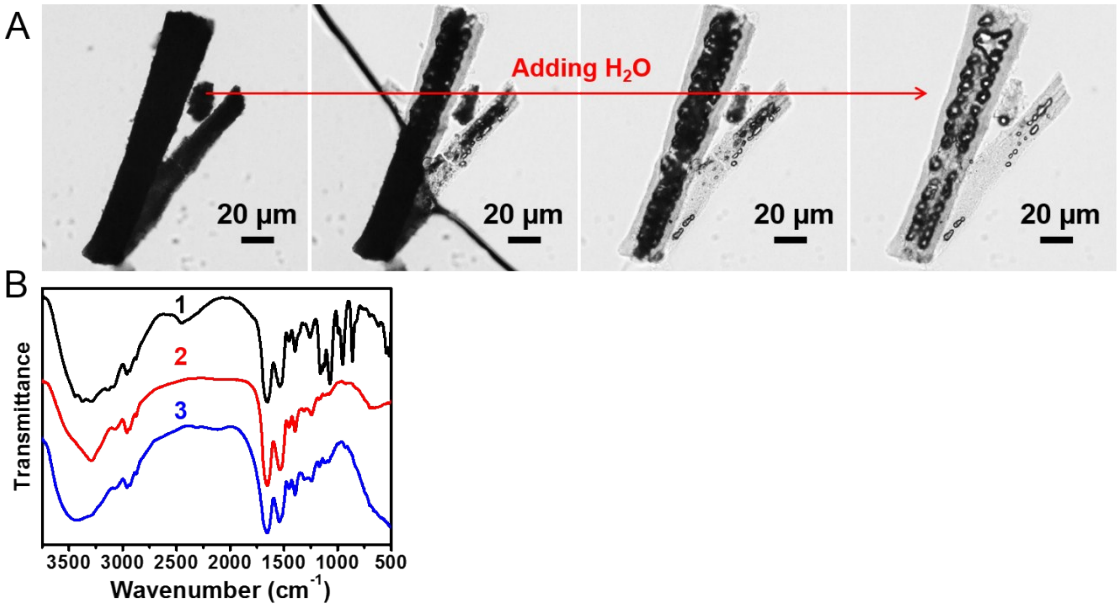

Figure S9. (A) Formation of BSA microtubes by gradually dissolving phosphate crystals in H_2O. (B) FTIR spectra of (1) phosphate crystal rods with shell of BSA fibrils, (2) cross-linked BSA microtubes after washing off phosphate crystal rods, and (3) BSA nanofibrils.

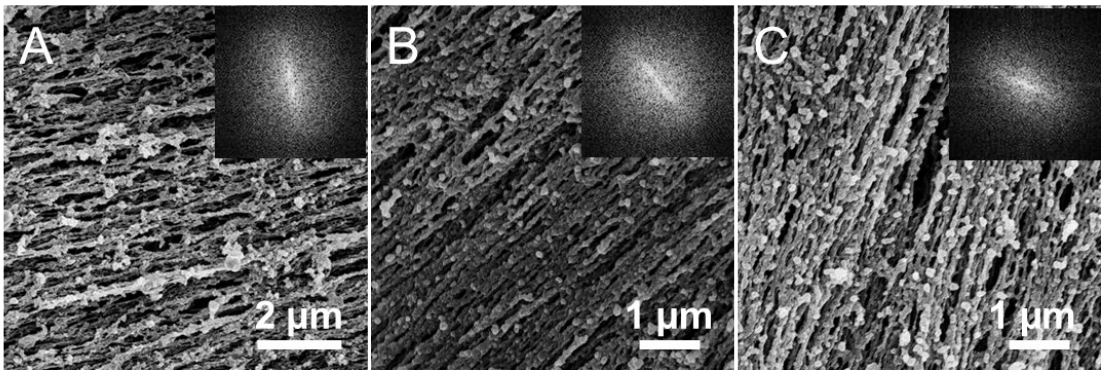

Figure S10. SEM images of BSA microtubes and corresponding Fast Fourier Transformation (the inset).

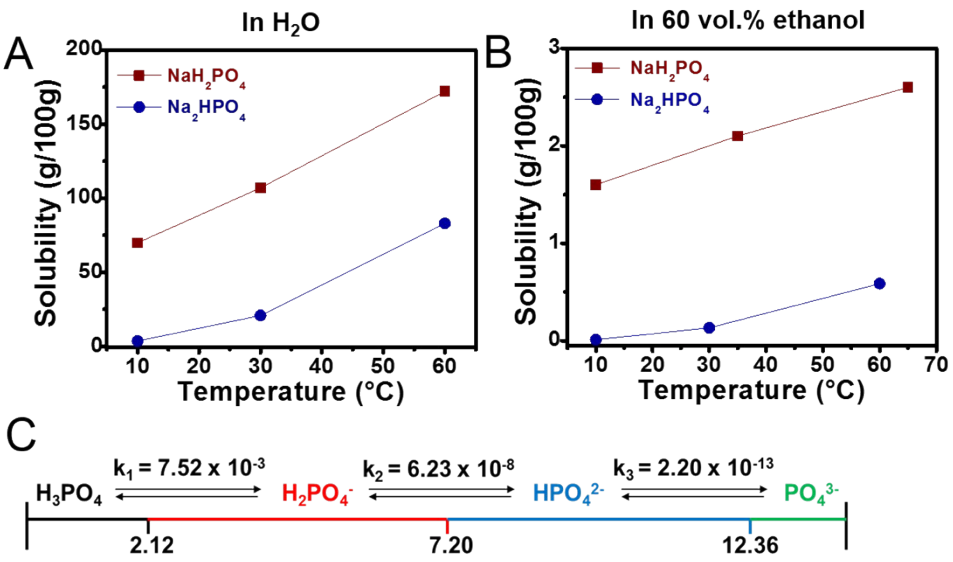

Figure S11. (A-B) Solubility of NaH_2PO_4 and Na_2HPO_4 in (A) H_2O and (B) 60 vol.% ethanol under various temperature. (C) Schematic illustration of the equilibrium between H_3PO_4, NaH_2PO_4, Na_2HPO_4 and Na_3PO_4 and the equilibrium constant for different pH values.

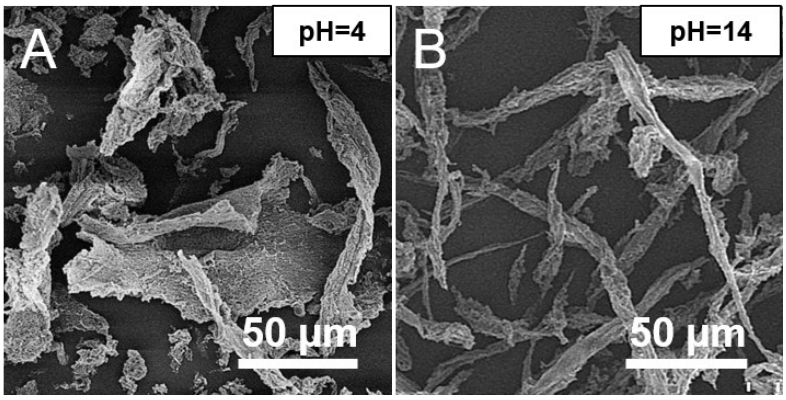

Figure S12. Aggregation of BSA fibrils synthesized when tuning the pH value at (A) pH 4 and (B) pH 14.

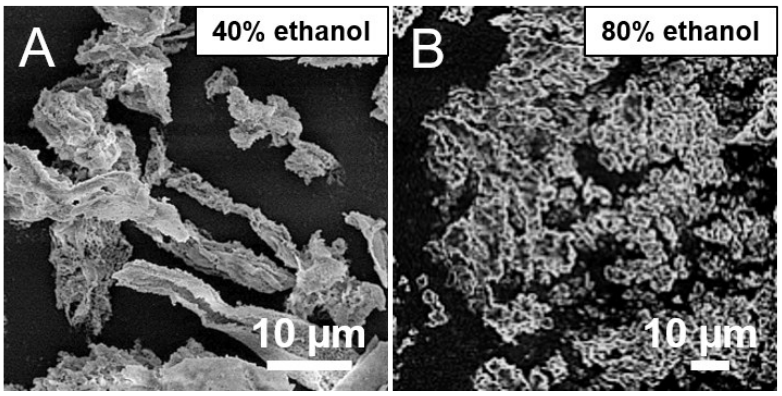

Figure S13. Aggregation of BSA fibrils synthesized when tuning the ethanol composition at (A) 40 vol.% and (B) 80 vol.%.

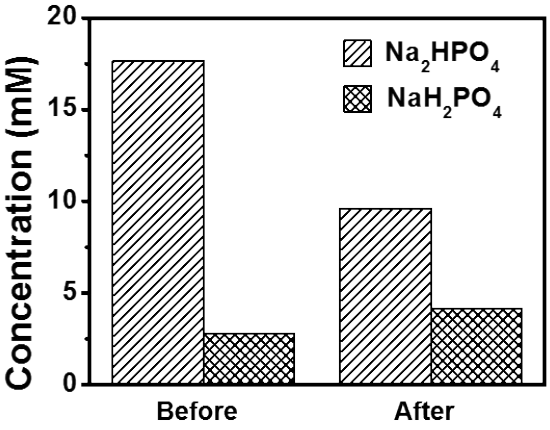

Figure S14. Variation of phosphate concentration before and after BSA fibrillation.

Sodium phosphate buffer (50 mM, pH 7.4) in 60 vol.% ethanol was directly measured as "Before". BSA was added, fibrillated, and removed by centrifugation, then the supernatant was measured as "After".

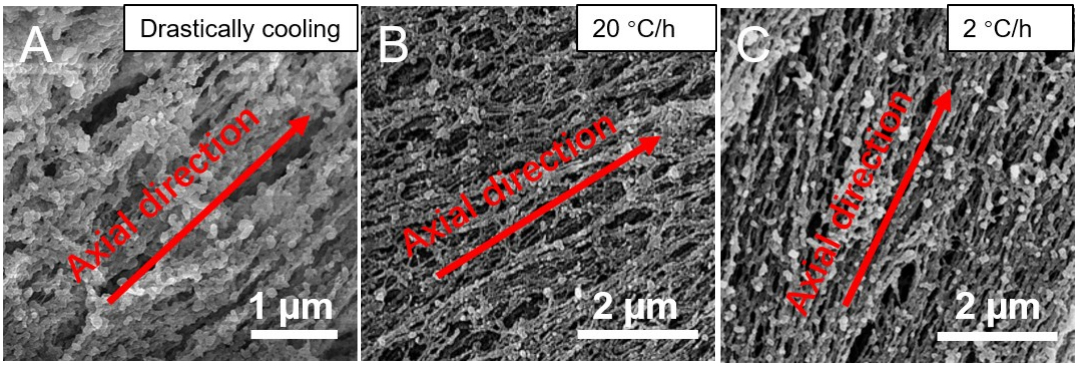

Figure S15. Different alignment of nanofibrils in BSA microtubes obtained at different cooling rates.

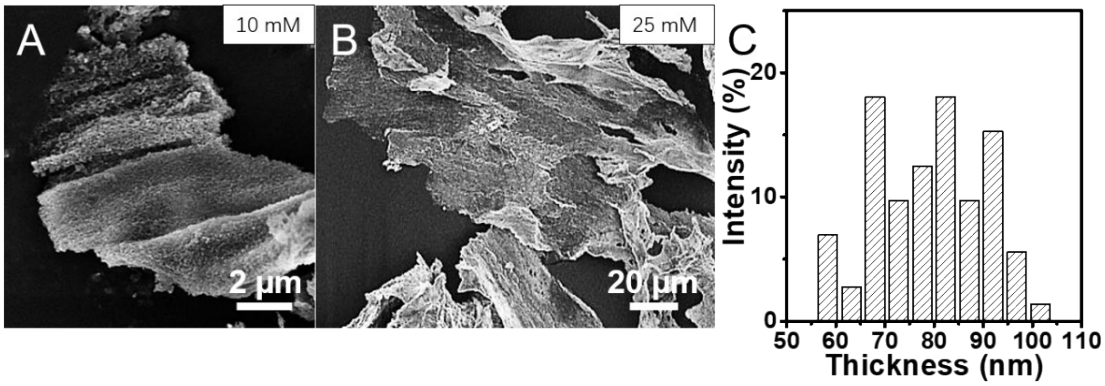

Figure S16. BSA nanosheets produced with initial phosphate concentrations of (A) 10 mM and (B) 25 mM. (C) Thickness distribution of BSA nanosheets.

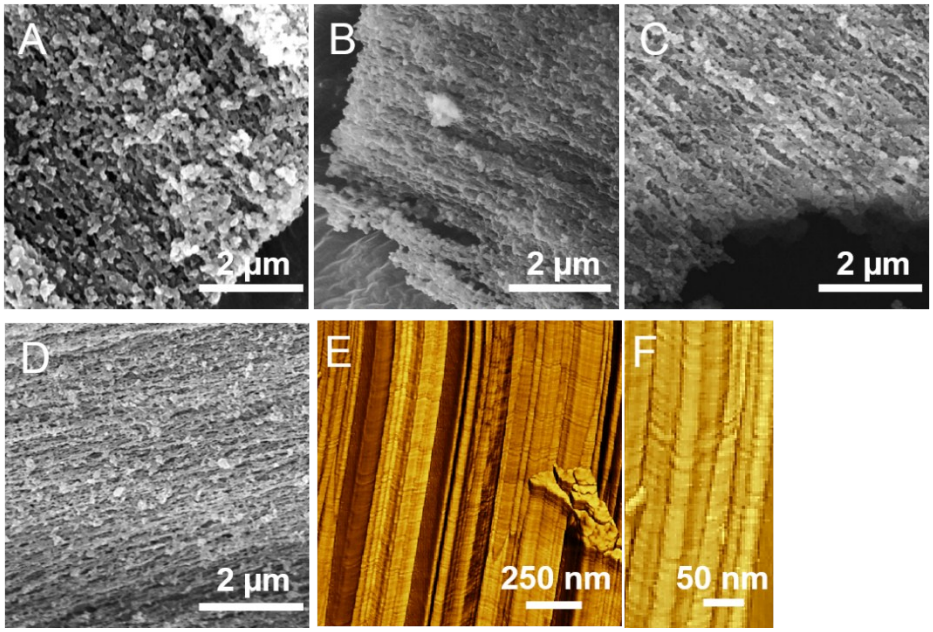

Figure S17. (A-D) SEM images and (E-F) AFM phase images of aligned nanofibrils on BSA nanosheets.

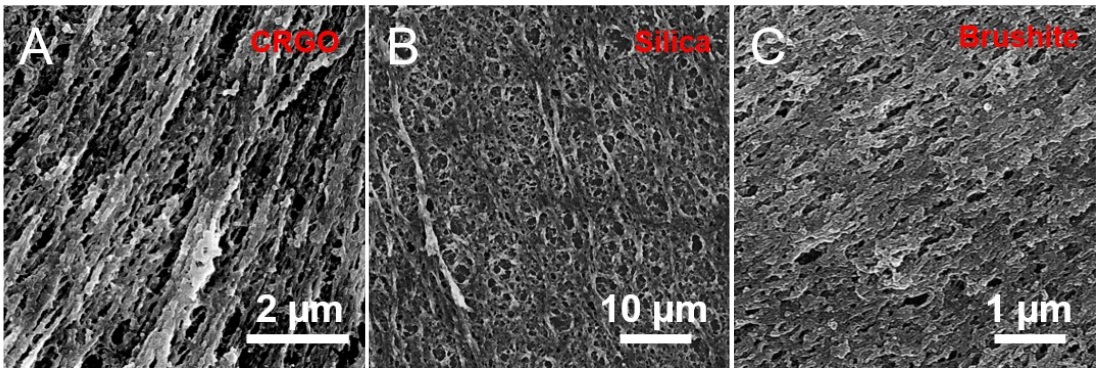

Figure S18. Aligning BSA fibrils on different substrates. (A) CRGO films, (B) silica wafer and (C) brushite platelets.

Preparation of chemically reduced graphene oxide (CRGO) films. Graphene oxide was synthesized using a modified Hummers method,[S4] and reduced to CRGO by ascorbic acid (50 mM) at 60 °C for 12 h. Then, CRGO was washed by H_2O for 3 times, filtrated on a 0.2 μm filter membrane, and dried at 60 °C for 2 days to get CRGO films.

Preparation of brushite platelets. 1.33 g $CaCl_2$ and 1.08 g NaH_2PO_4 were dissolved in 200 mL of CH_3COONa solution (30 mM, pH ~ 5), respectively. After mixing the two solutions, the reaction continued at 60 °C for 12 h. The products were washed, filtered and dried at 60 °C overnight to get the brushite platelets.

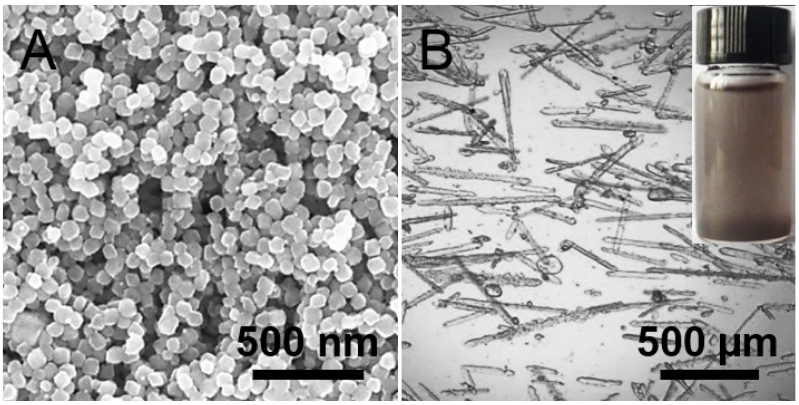

Figure S19. (A) SEM images of Fe_3O_4 nanoparticles. (B) BSA microtubes with Fe_3O_4 nanoparticles attached.

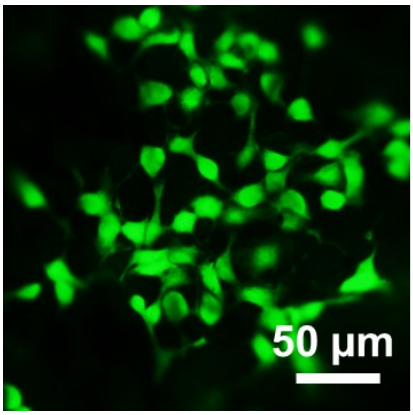

Figure S20. Microphotograph image of Hela cells cultured on coverslips.

RERERENCE

S1. Wang, L.; Bao, J.; Wang, L.; Zhang, F.; Li, Y. One-Pot Synthesis and Bioapplication of Amine-Functionalized Magnetite Nanoparticles and Hollow Nanospheres. *Chem–Eur. J.* **2006,** *12*, 6341-6347.

S2. Wu, X.; Li, M.; Li, Z.; Lv, L.; Zhang, Y.; Li, C. Amyloid-graphene Oxide as Immobilization Platform of Au Nanocatalysts and Enzymes for Improved Glucose-sensing Activity. *J. Colloid Interface Sci.* **2017,** *490*, 336-342.

S3. Ling, S.; Li, C.; Adamcik, J.; Wang, S.; Shao, Z.; Chen, X.; Mezzenga, R. Directed Growth of Silk Nanofibrils on Graphene and Their Hybrid Nanocomposites. *Acs Macro Lett.* **2014,** *3*, 146-152.

S4. Wu, X.; Zhang, Y.; Han, T.; Wu, H.; Guo, S.; Zhang, J. Composite of Graphene Quantum Dots and Fe_3O_4 Nanoparticles: Peroxidase Activity and Application in Phenolic Compound Removal. *Rsc Adv.* **2014,** *4*, 3299-3305.